Electronic Supplementary Material (ESI) for Sustainable Energy & Fuels.

Perceiving the temperature coefficients of carbon-based perovskite solar cells

Shubhranshu Bhandari,*[a] Anurag Roy,[a] Aritra Ghosh,[a] Tapas Kumar Mallick[a] and Senthilarasu Sundaram*[a]

[a]Environment and Sustainability Institute (ESI), Penryn Campus, University of Exeter, Cornwall, TR10 9FE, U.K.

* Corresponding authors

E-mail: sb964@exeter.ac.uk, s.sundaram@exeter.ac.uk

Supplementary note 1: Performance evaluation of the as-prepared S_T c-PSC devices made in ambient conditions in the temperature range of 5 °C to 75 °C. Fig. S1 suggests 25 °C is the most suitable for the working ability of devices in S_T conditions. The average integrated photocurrent densities of S_T c-PSCs are given in Table S1 along with the EIS spectra fitting data.

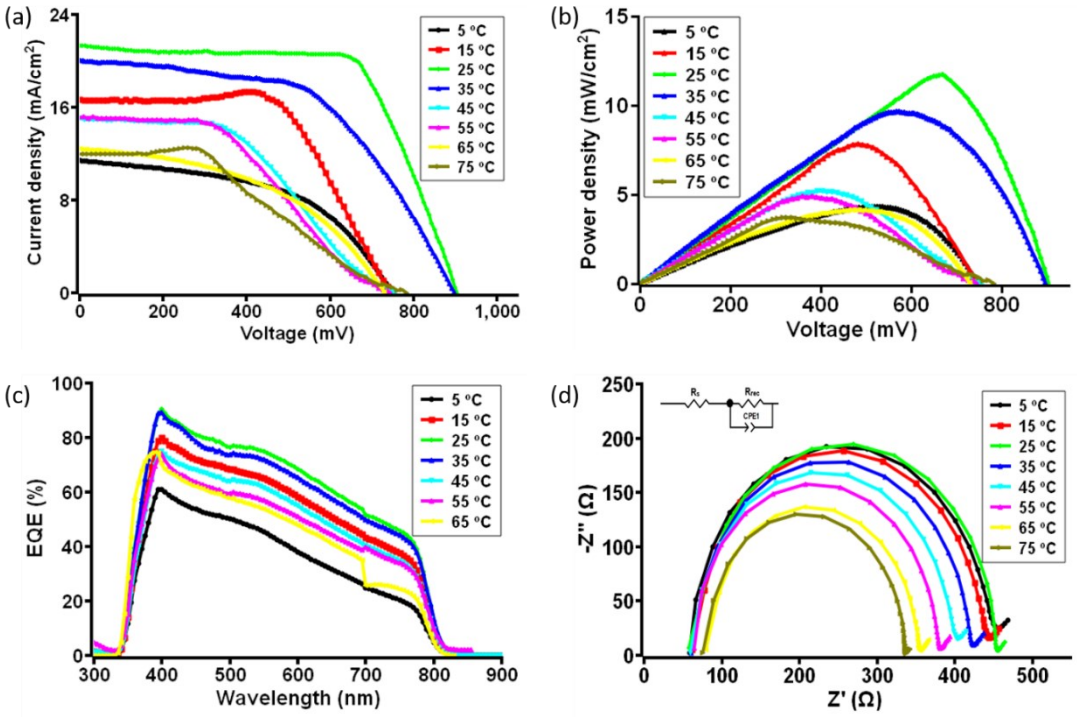

Fig. S1 (a) Current density – voltage *(J-V)* curves and (b) power density - voltage curve for the S_T PSCs at different temperatures in the range of 5 °C to 75 °C, (c) IPCE spectra of c-PSCs at different temperatures, and (d) corresponding EIS characteristics (Nyquist plots) with the fitted circuit diagram for S_T devices having the best performance.

Table S1 Integrated photocurrent density values of S_T devices at different temperatures calculated from IPCE, and EIS spectra fitting data of respective devices.

Temperature (°C)	**Integrated J_{SC} ($mA.cm^{-2}$)**	**R_S (Ω)**	**R_{rec} (Ω)**
5	9.75	58.19	380.6
15	14.6	59.47	374.1
25	20	54.36	343
35	16.43	60.13	357.3
45	13.69	59.07	335.3
55	13.0	61.34	315.7
65	11.85	78.88	273
75	11.02	75.54	207.5

Supplementary note 2: Photovoltaic performance variation at different temperature is given in Fig. S2 for S_T condition. The variation was observed for five devices at a particular temperature.

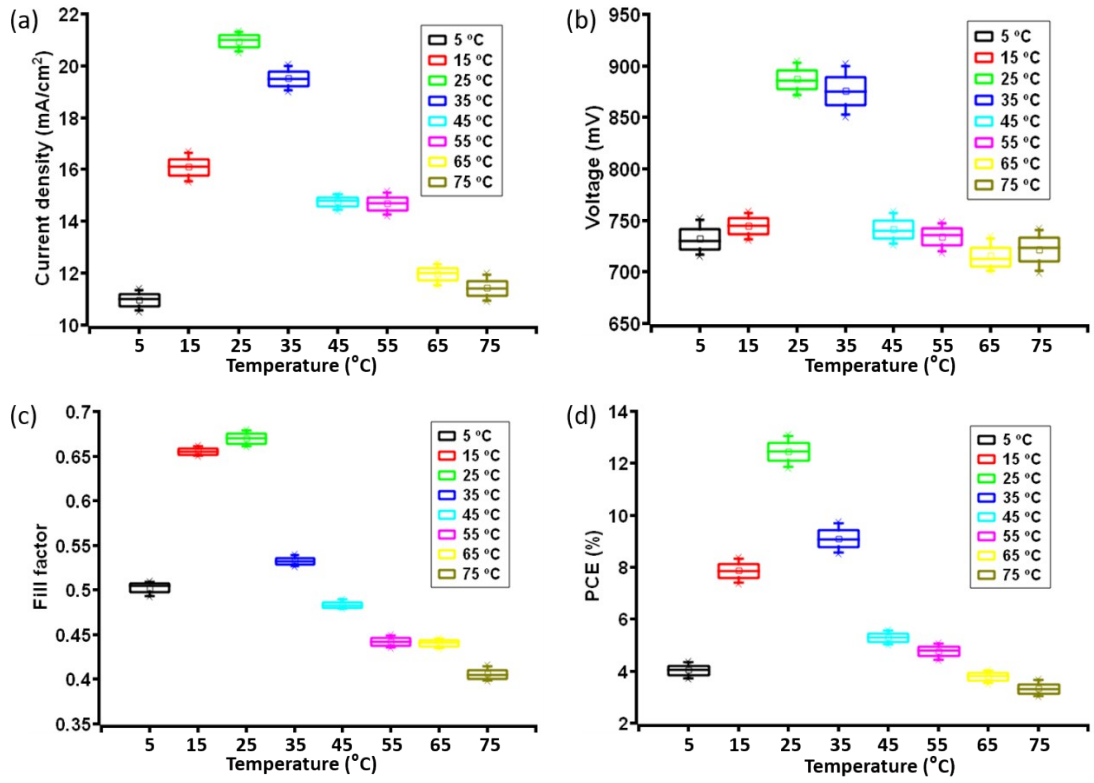

Fig. S2 Photovoltaic characterization of three randomly picked S_T devices for each temperature in the range of 5 °C to 75 °C. Box and whiskers plot of current density vs. temperature (a), voltage vs. temperature (b), Fill factor vs. temperature (c), and PCE vs. temperature (d), respectively.

Supplementary note 3: Performance evaluation of the as-prepared T_T c-PSC devices made in ambient conditions in the temperature range of 5 °C to 75 °C. The Fig. S3 suggests 15 to 35 is the most suitable for the effectiveness of devices. The average integrated photocurrent densities of T_T c-PSCs are given in Table S2 along with the EIS spectra fitting data.

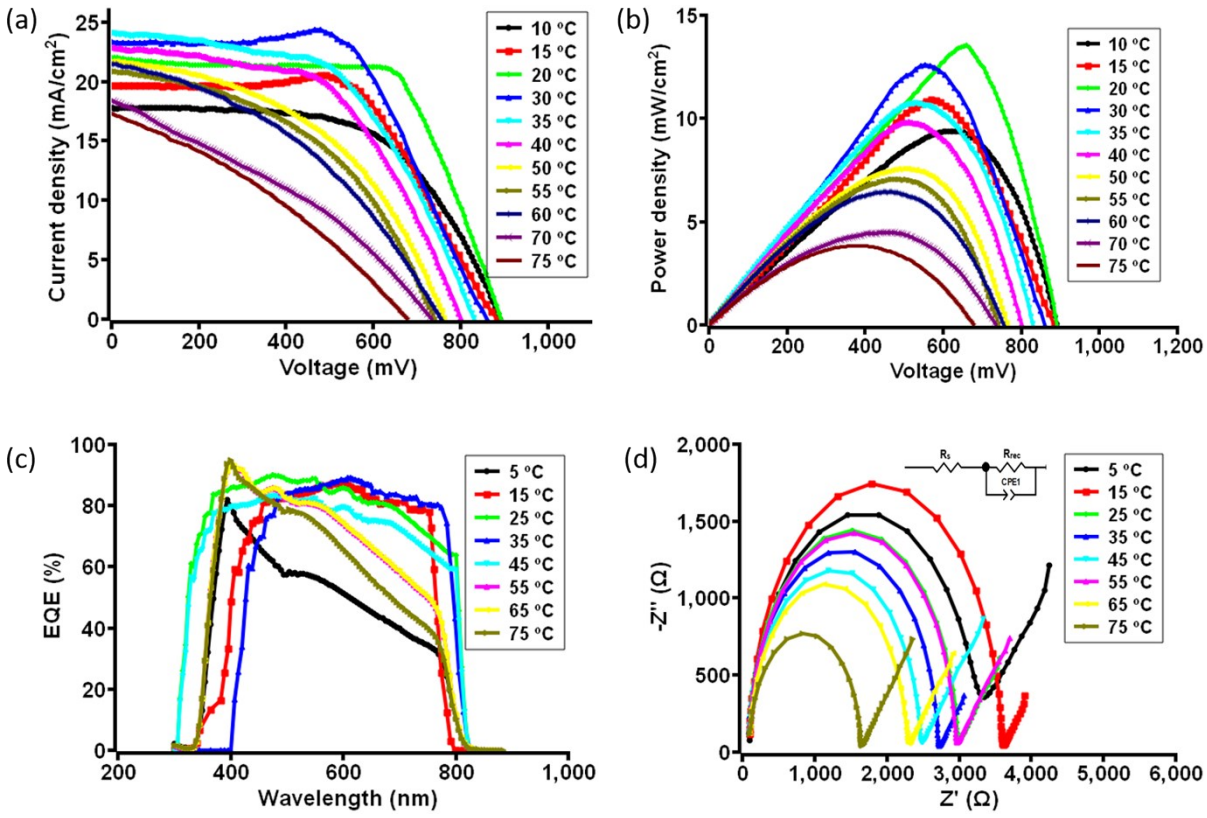

Fig. S3 (a) Current density - voltage curves and (b) power density - voltage curve for the T_T PSCs at different temperatures in the range of 5 °C to 75 °C, (c) IPCE spectra of c-PSCs at different temperatures, and (d) corresponding EIS characteristics (Nyquist plots) with the fitted circuit diagram for T_T devices having the best performance.

Table S2 Integrated photocurrent density values of T_T devices at different temperatures calculated from IPCE, and EIS spectra fitting data of respective devices.

Temperature (°C)	**Integrated J_{SC} ($mA.cm^{-2}$)**	**R_S (Ω)**	**R_{rec} (Ω)**
5	13.1	96.9	3015
15	18.5	77.55	2936
25	21	66.37	1599
35	22.4	89.18	2619
45	20.7	89.2	2359
55	18.4	94.32	2844
65	17.1	94.72	2171
75	16.5	93.62	1536

Supplementary note 4: Photovoltaic performance variation at different temperature is given in Fig. S4 for T_T condition. The variation was observed for five devices over the entire range of temperature.

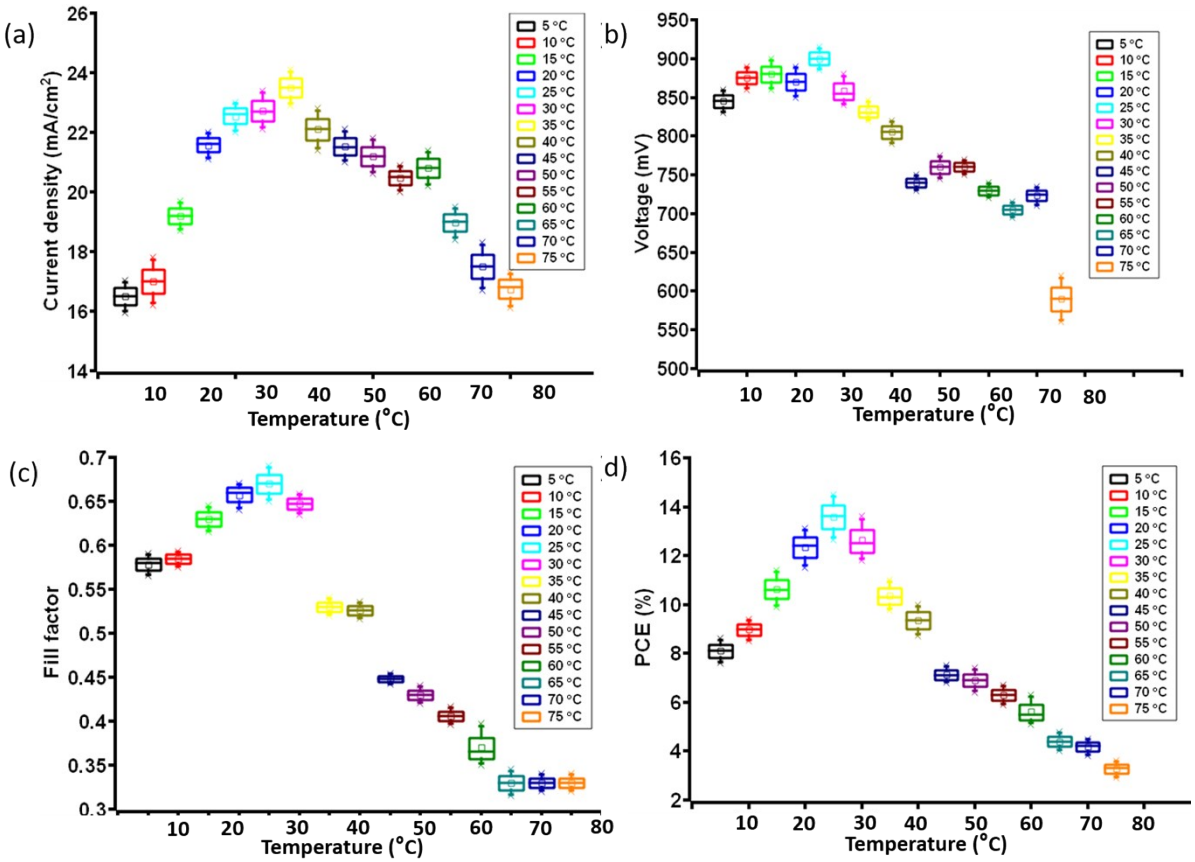

Fig. S4 Photovoltaic characterization of three randomly picked T_T devices for each temperature in the range of 5 °C to 75 °C. Box and whiskers plot of current density vs. temperature (a), voltage vs. temperature (b), Fill factor vs. temperature (c), and PCE vs. temperature (d), respectively.

Supplementary note 5: The full cycle of temperature treatment for the champion device in temperature range of 5 to 75 °C is shown in Fig. S5. It shows a reversible nature of T_T testing devices.

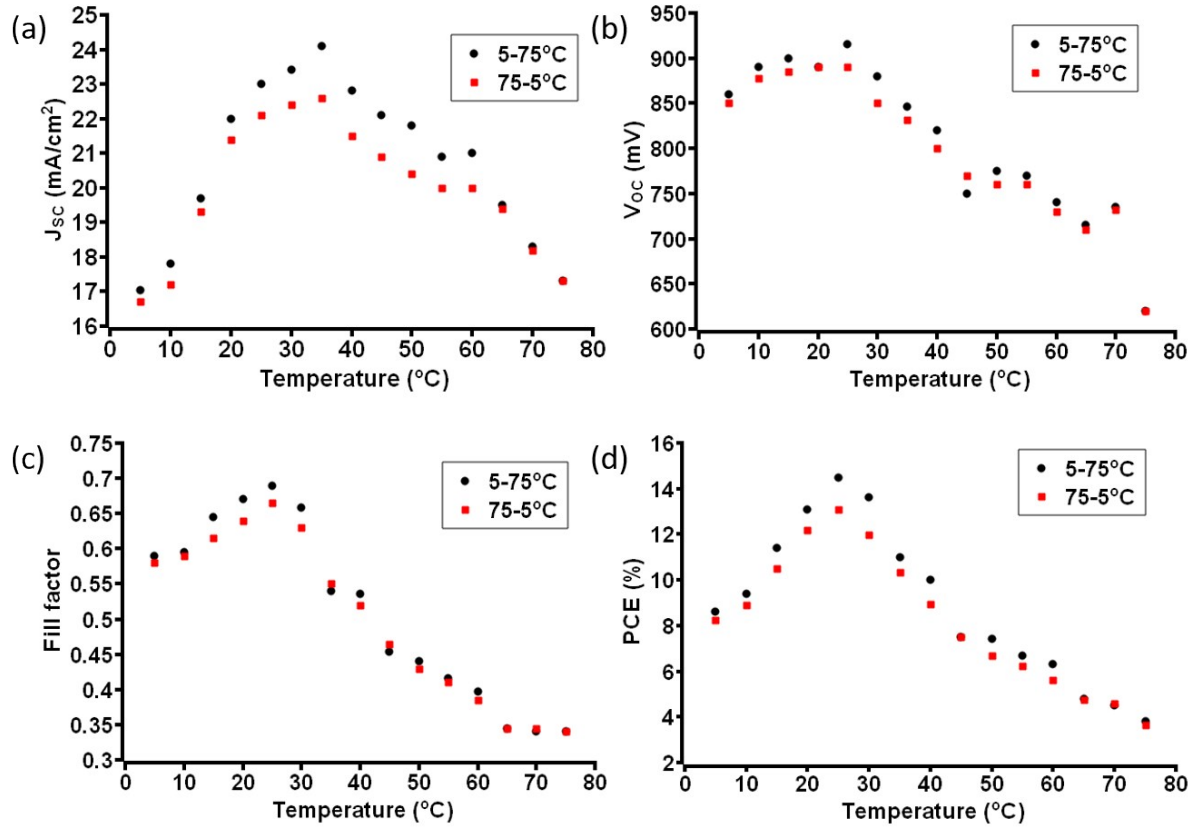

Fig. S5 The reversible nature of the parameters of champion device in TT testing conditions.

Supplementary note 6: XRD plot shown in Fig. S5 dictates the formation PbI_2 at low and high temperature zones. The extent of degradation is more at high temperature region. The degradation of perovskite does not form any kind of composites with Al_2O_3. Although higher rate of degradation at around 75 °C suggest favourable interaction between $Al2O_3$ and PbI_2.

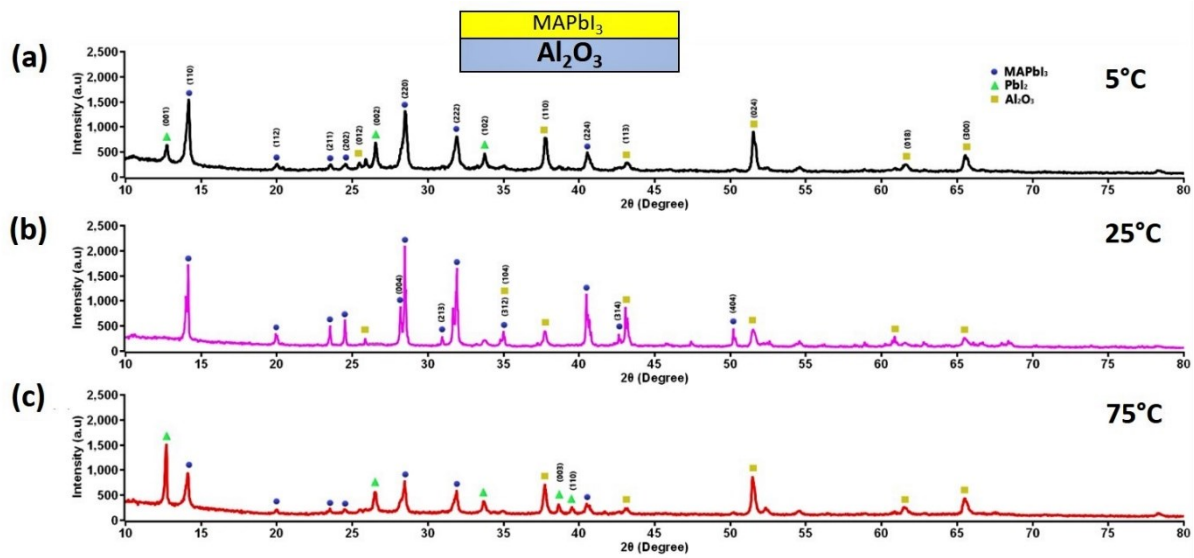

Fig. S6 XRD data of Al_2O_3 and perovskite at 5, 25, and 75 °C, respectively.

Supplementary note 7: The XRD plot given in Fig. S6 shows the presence of anatase and rutile phase of TiO_2 for all three temperature conditions. The extent of perovskite degradation in low anh high temperature is almost similar. No trace of composite formation was found.

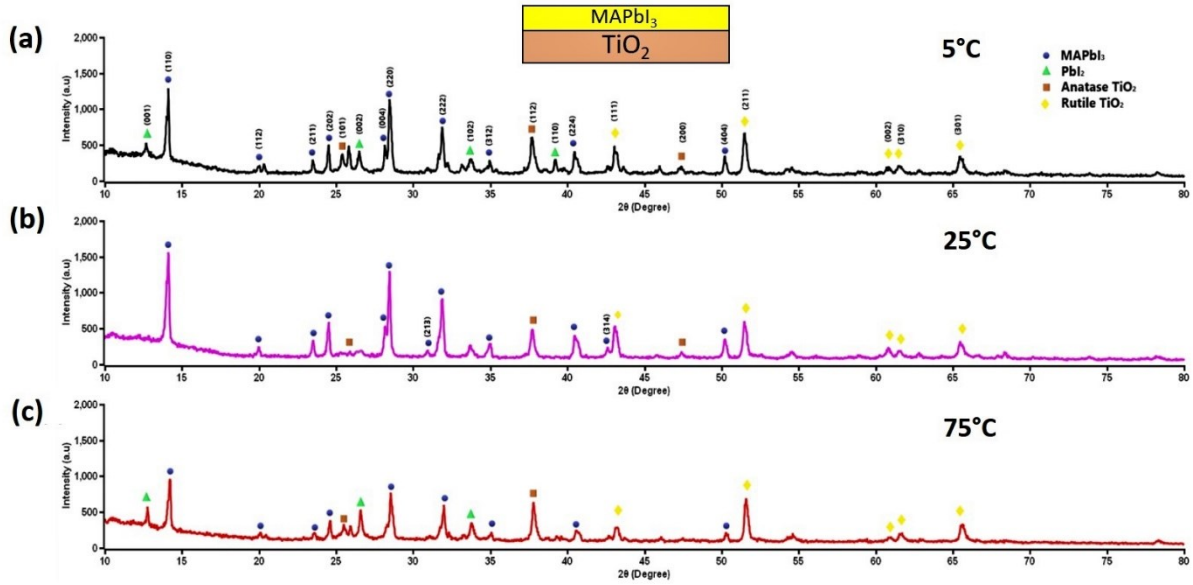

Fig. S7 XRD data of with TiO_2 and perovskite at 5, 25, and 75 °C, respectively.

Supplementary note 8: Fig. S6 demonstrates top surface FESEM images showing the formation of composite material with carbon depending on temperature. At 25 °C (Fig. S6c), fine particle structure of the carbon electrode with perovskite can be seen. On the other hand, Fig. S6b and S6d claim the formation of composite in moving towards lower and higher temperatures from 25 °C.

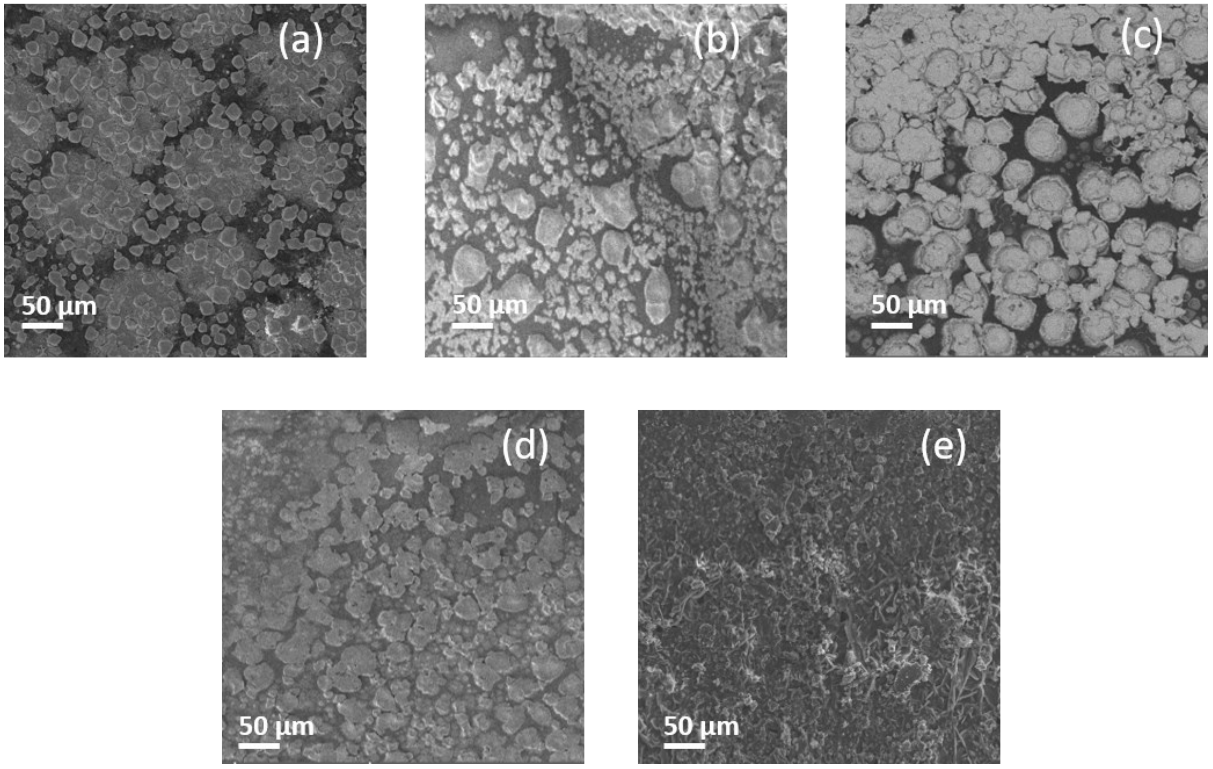

Fig. S8 (a) Top surface SEM of S_T devices at 5 °C, (b) top surface FESEM of S_T devices at 15 °C, (c) top surface SEM of S_T devices at 25 °C, (d) top surface FESEM of S_T devices at 45 °C, and (e) top surface SEM of S_T of devices at 75 °C.